Lipid metabolic reprogramming drives triglyceride storage and variable sensitivity to FASN inhibition in endocrine-resistant breast cancer cells

Ashley V. Ward[1], Duncan Riley[1], Kirsten E. Cosper[1], Jessica Finlay-Schultz[1], Heather M. Brechbuhl[2], Andrew E. Libby[3], Kaitlyn B. Hill[4], Rohan R. Varshney[4], Peter Kabos[2], Michael C. Rudolph[3#], and Carol A. Sartorius[4#*]

[1] University of Colorado, Anschutz Medical Campus; Department of Pathology; Aurora, CO, United States. (ashley.2.ward@cuanschutz.edu)

[2] University of Colorado, Anschutz Medical Campus; School of Medicine; Division of Medical Oncology; Aurora, CO, United States.

[3] University of Colorado, Anschutz Medical Campus; School of Medicine; Division of Endocrinology; Aurora, CO, United States.

[4] University of Oklahoma Health Sciences Center, Harold Hamm Diabetes Center; Oklahoma City, OK, United States.

# these authors contributed equally

*Correspondence

Carol A Sartorius

Carol.Sartorius@cuanschutz.edu

Key words: Breast cancer; endocrine resistance, lipid metabolism; fatty acid; lipidomics; fatty acid synthase

Abstract

Background: Lipid metabolic reprogramming is increasingly recognized as a hallmark of endocrine resistance in estrogen receptor-positive (ER+) breast cancer. In this study, we investigated alterations in lipid metabolism in ER+ breast cancer cell lines with acquired resistance to common endocrine therapies and evaluated the efficacy of a clinically relevant fatty acid synthase (FASN) inhibitor.

Methods: ER+ breast cancer cell lines resistant to Tamoxifen (TamR), Fulvestrant (FulvR), and long-term estrogen withdrawal (EWD) were derived. Global gene expression and lipidomic profiling were performed to compare parental and endocrine resistant cells. Lipid storage was assessed using Oil Red O (ORO) staining. The FASN inhibitor TVB-2640 was tested for its impact on lipid storage and cell growth. $^{13}C_2$-acetate tracing was used to evaluate FASN activity and the efficacy of TVB-2640.

Results: Endocrine resistant cells showed significant enrichment in lipid metabolism pathways and distinct lipidomic profiles, characterized by elevated triglyceride levels and enhanced cytoplasmic lipid droplets. $^{13}C_2$-acetate tracing revealed increased FASN activity in endocrine resistant cells, which was effectively reduced by TVB-2640. While TVB-2640 reduced lipid storage in most but not all cell lines, this did not correlate with decreased cell growth. Polyunsaturated fatty acids (PUFAs) containing 6 or more double bonds were elevated in endocrine resistant cells and remained unaffected or increased with TVB-2640.

Conclusion: Endocrine resistant breast cancer cells undergo a metabolic shift toward increased triglyceride storage and PUFAs with high degrees of desaturation. While TVB-2640 reduced lipid storage in most conditions, it had limited effects on the growth of endocrine resistant breast cancer cells. Targeting specific lipid metabolic dependencies, particularly pathways that produce PUFAs, represents a potential therapeutic strategy in endocrine resistant breast cancer.

Background

Overcoming resistance to endocrine therapies represents a pivotal challenge for enhancing treatment outcomes in women with estrogen receptor-alpha (ER) positive breast cancer, contributing to approximately half of all fatalities from the disease (1). The three most common classes of drugs used during endocrine therapy include selective ER modulators (SERMS, e.g., Tamoxifen, (Tam)) that disrupt binding of estrogens to ER, selective ER degraders (SERDs, e.g., Fulvestrant (Fulv)) that cause immobilization and/or degradation of ER (2), and aromatase inhibitors that block production of 17β-estradiol. Typically administered as adjuvant therapy for over 5-10 years, endocrine therapy offers long-term disease stabilization or eradication for most patients. Unfortunately, acquired endocrine resistance emerges in up to one third of women either during treatment or upon its conclusion, often coinciding with distal metastasis (3). At this time, several targeted therapies may be integrated in combination with endocrine therapy, including cyclin dependent kinases 4/6 inhibitors (i.e. palbociclib), alpelisib for PIK3CA mutations, or the SERD elacestrant for tumors harboring ER mutations (4, 5). However, the development of acquired multidrug resistance is usually inevitable. Consequently,

69 an urgent need exists to identify new vulnerabilities in endocrine resistant cells that can be
70 effectively targeted in combination with endocrine drugs to mitigate the recurrence risk or delay
71 progression of recurrent disease.

72 ER+ breast cancers exhibit pronounced lipogenesis, utilizing de novo fatty acid (FA)
73 synthesis despite the presence of abundant FAs in their microenvironment (6). FAs originating
74 from preformed sources facilitate synthesis of more complex lipids necessary for membrane
75 expansion, provide fuel for rapid tumor growth, and act as signaling molecules. Central to this
76 process is the upregulation of Sterol Regulatory Element-binding transcription factor 1
77 (SREBP1) by estrogens, which in turn boosts the expression of two vital de novo FA synthesis
78 enzymes necessary in this pathway: acetyl-CoA carboxylase (ACC) and fatty-acid synthase
79 (FASN) (7). ACC catalyzes the conversion of acetyl-CoA into malonyl-CoA, and both precursors
80 are needed for further catalysis by FASN to synthesize palmitate. Palmitate and further elongated
81 FAs are subsequently combined with preformed FA taken up from the microenvironment by
82 transporters, and together, they are subsequently incorporated into triglycerides and frequently
83 stored as cytoplasmic lipid droplets (LD) in breast cancer cells (8-10). This dual mode of FA
84 synthesis and FA uptake underscores the complexity of targeting FA dependence in breast
85 cancers, especially given the adaptability in the metabolic incorporation of these essential
86 molecules that provide an advantage to cancer cells.

87 Recent studies have shown that lipid metabolic pathways undergo further alteration with
88 the development of endocrine resistance, with a significant body of research centering on Tam,
89 the longest approved breast cancer drug (11). Hultsch et al. observed that Tam-resistant breast
90 cancer cells had a significant increase in triglycerides and cholesterol esters, stored in large LDs
91 and lysosomes, respectively (12). Moreover, ER+ invasive lobular carcinoma cells, resistant to

92 long term estrogen deprivation, exhibited heightened activation of lipid metabolism that could be
93 stratified into two distinct lipid pathways, SREPB1-activated FA synthesis or cholesterol
94 metabolism (13). Notably, MCF7 cells subjected to long-term estrogen deprivation experience an
95 uptick in cholesterol biosynthesis (14). HER2-overexpressing MCF7 variants had elevated FASN
96 expression alongside an increased dependency on lipid biosynthesis (7).

97 While multiple potential targets within lipid metabolism are promising, FASN inhibition
98 has historically received the most attention. FASN levels are consistently higher in breast cancer
99 compared to normal cells and breast tumor vs normal tissue (15). While early-generation FASN
100 inhibitors demonstrated potential efficacy for tumor growth restriction in preclinical breast
101 cancer models, their clinical translation was limited due to substantial toxicity observed in both
102 animal models and human trials (16). However, a more recently developed selective and
103 reversible FASN inhibitor (TVB-2640) has shown promising results, including dose-dependent
104 efficacy in advanced solid tumors like HER2-positive breast cancers and has advanced to Phase
105 II clinical trials (17). Beyond FASN, other targets within lipid metabolism are currently being
106 explored, such as inhibitors of fatty acid oxidation (FAO), fatty acid transport, and the synthesis
107 of monounsaturated fatty acids (18). Given the possibility for compensation within lipid
108 metabolic pathways, therapeutic strategies targeting single enzymes are usually met with
109 metabolic adaptations, suggesting combinatorial approaches using established drugs might yield
110 stronger outcomes.

111 In this study, we analyzed the global lipidome of breast cancer cells exhibiting resistance
112 to three common endocrine therapy modalities. Our findings reveal that while the lipid
113 composition of endocrine resistant cells is distinct from each other and from their endocrine
114 sensitive counterparts, they share an increased abundance of triglycerides, LDs and complex

115 lipids containing highly polyunsaturated FA (PUFA) species. The FASN inhibitor TVB-2640
116 effectively blocked FASN activity, but showed variable effects on lipid storage and cell growth,
117 with only modest reductions observed in some resistant subtypes. Furthermore, certain endocrine
118 treatments enhanced PUFA levels when FASN was inhibited. These results underscore the
119 distinct lipid metabolism signature of endocrine resistant breast cancer cells and highlight the
120 challenges of targeting FASN in endocrine resistance. Importantly, a reliance on lipid
121 desaturation pathways emerges as a potential vulnerability in endocrine resistance.
122
123
124 **Materials and Methods**
125
126 **Generation of Endocrine Therapy Resistant Cell Lines**
127 T47D cells were maintained in minimal Eagle's medium supplemented with 5% fetal bovine
128 serum (FBS), 1x non-essential amino acids (NEAA), 1 nM insulin, and 1 mM sodium pyruvate
129 unless otherwise noted. The generation and characterization of breast cancer patient-derived
130 xenograft (PDX)- derived cell lines UCD4 and UCD65 was previously described (19). UCD4
131 and UCD65 cells were maintained in Dulbecco's Modified Eagle Media/F-12 (50:50)
132 supplemented with 10% FBS, 100 ng/mL choleratoxin, and 1 nM insulin. Cell lines were
133 authenticated by short tandem repeat analysis and routinely tested for mycoplasma using the
134 MycoAlert mycoplasma detection kit (Lonza, #LT07-710). UCD4 contains an ESR1 mutation
135 (D538G).
136 To establish endocrine resistant variants, cells were exposed to escalating doses of ICI 182780
137 (Fulv, Faslodex, T47D and UCD4) or 4-hydroxytamoxifen (4OHT, Tam, T47D, UCD4, and

138 UCD65) over a 12-month period to establish endocrine resistance. The starting dose for Fulv and
139 Tam were 10 times lower than the effective dose for each compound, 1 nM and 10 nM
140 respectively. Both compounds were dissolved in 100% EtOH to make stock concentrations that
141 resulted in the final dose being less than 0.1% EtOH. Fulv resistant (FulvR) and Tam resistant
142 (TamR) cells were maintained at established resistance concentrations, 100 nM and 1 μM,
143 respectively. For estrogen withdrawal, UCD4 cells (UCD4-EWD), were cultured for 12-months
144 in phenol-red free media supplemented with charcoal stripped serum.
145
146 **RNA-sequencing**
147 Parental and resistant cells were plated in 6-well plates at $5x10^5$ (T47D) or $1x10^6$ (UCD4)
148 cells/well in normal media conditions with appropriate maintenance Fulv or 4OHT drug
149 concentrations. All samples were grown to 80% confluency then harvested until all samples were
150 ready for processing. RNA was isolated using QIAzol lysis reagent (Qiagen, #79306) and
151 RNAeasy Mini Kit (Qiagen, #74104) and treated with RNase-free DNase (Qiagen, #79254).
152 Libraries were prepared by the University of Colorado Genomics Shared Resource using
153 Illumina TruSeq Stranded mRNA Library Prep kit (Illumina, #20020595) and sequenced using
154 paired end 50 cycles 2 x 50 on the NovaSEQ 6000 with >30 million reads per sample obtained.
155 Paired-end 150 nucleotide reads were aligned to the human genome version GRCh38.p13 using
156 STAR. Downstream expression analysis was performed using Cufflinks. The resulting aligned
157 files (BAM) were then used to infer the differentially expressed gene profiles using DESeq2.
158 Over representation analysis (ORA) was performed using the Gene Ontology (GO) Cellular
159 Component gene set collection via WebGestalt (20).
160

161 **Unbiased Lipid Mass Spectrometry**

162 $1x10^6$ cells were plated in 6 cm plates in normal media conditions (N=4 per condition).
163 Maintenance Fulv and 4OHT drug concentrations were added to resistant cell line plates. Cells
164 were harvested at 80% confluency. Modified MTBE liquid-liquid extraction was used with a
165 protein crash. The lipid fraction was reconstituted in 100 µL Methanol. The aqueous fraction was
166 reconstituted in 50 µL 5% Acetonitrile in water. The lipid fraction was run in positive ionization
167 mode on the Agilent 6560 IMMS-QTOF, in QTOF-only mode (Analytical column: Agilent
168 Zorbax Rapid Resolution HD (RRHD) SB-C18, 1.8 µm, 2.1x100 mm; column temp 60C;
169 Gradient elution: 0–0.5 minutes 30–70% B, 0.5–7.42 minutes 70–100% B, 7.42–9.9 minutes
170 100% B, 9.9–10.0 minutes 100–30% B, 10–14.6 minutes 30% B; Flow rate 0.6mL/min; Mobile
171 phase A: water with 0.1% formic acid; Mobile phase B: 60:36:4 isopropyl
172 alcohol:acetonitrile:water with 0.1% formic acid). Spectral peaks were extracted using Mass
173 Hunter Profinder version B.08.00 using a Recursive Workflow and area-to-height conversion.
174 Data were normalized using Total Useful Signal (TUS) where an abundance ratio is calculated
175 for each compound and the average of the ratio for all compounds becomes the normalization
176 factor. Final data are thus "normalization target abundance/run abundance" (21). The final
177 spectral data were imported into Mass Profiler Professional (MPP) version 14.9 filtered to be
178 present in at least 2 out of the 16 samples. Annotation was performed using our in-house Mass
179 and Retention Time (MSRT) database, HMDB databases, Lipid Maps database, KEGG
180 databases, and a Metiln database. MetaboAnalyst and LION were used to generate significant
181 pathways, based on an ANOVA-computed annotated list of compounds. Only pathways with >2
182 compounds in the set were reported. Unsaturated lipid species were calculated from results using
183 total abundance.

184

185 **Targeted Lipid Mass Spectrometry**

186 For $^{13}C_2$-acetate tracer studies, $4x10^5$ cells were plated in 6 well plates in normal media
187 conditions (N=3 per condition). Maintenance Fulv and 4OHT drug concentrations were added to
188 resistant cell line plates. Cells were treated with 10 µM TVB-2640 or DMSO for 72 hr. After 24
189 hr of FASN inhibition or vehicle treatment, all wells were supplemented with 250 µM 13C-2
190 acetate for a 48 hr tracer incubation. Cells were harvested with trypsin, pelleted, and flash frozen
191 in liquid nitrogen. Flash frozen cell pellets were lysed in 1ml 66% methanol (vol/vol) in 0.1M
192 potassium phosphate buffer, pH 6.8 by vigorously vortexing twice with 20 second pulses.
193 Reserving 10ul from these lysates, total cellular protein estimation was done using BCA assay
194 (Thermo Fisher, #23225). The remainder of the lysates were then transferred to 13x100 mm
195 borosilicate glass culture tubes (Fisher Scientific, #14-961-27). Lysates were acidified with 10ul
196 of 1N HCl (prewashed with Hexanes) and vortexed briefly. Total lipids were extracted twice by
197 adding 1mL of isooctane:ethyl acetate 3:1 (vol/vol) and once with 1mL Hexanes; for each
198 extraction, samples were vortexed vigorously for 10-15 sec and centrifuged at 2000g for 1
199 minute to complete phase separation. The upper organic layer from each extraction was
200 combined into a new 13x100 mm borosilicate glass tube. Extracted lipids were brought to
201 dryness and resuspend in 300 ul 2,2,4-Trimethylpentane (isooctane). For the non-esterified FA
202 (NEFA) fraction, 100 ul of the resuspended total lipids was transferred to a new borosilicate
203 glass tube, mixed with (30 ng) blended stable isotope internal standard, taken to dryness under
204 gaseous N_2, and resuspended in 25ul of 1% pentafluorobenzyl bromide in acetonitrile (vol/vol),
205 to which 25 ul of 1% diisopropylethylamine in acetonitrile (vol/vol) was added, and samples
206 were incubated at room temperature for 30 minutes. Pentafluorbenzyl-FA derivatives were taken

207 to dryness under gaseous N_2 and resuspended in 120ul hexanes of injection into the GC/MS. For
208 the total fatty acid fraction (TFA), 20ul of the original 300 uL total lipid extract was transferred
209 to a separate Teflon lined screw cap glass tube, mixed with (66.7 ng) blended stable isotope
210 internal standard, and taken to dryness under gaseous N_2. TFA samples were resuspended in 500
211 ul of 100% ethanol to which 500 ul of 1M NaOH was added to saponify the TFA fraction at 90C
212 for 30 minutes, followed by acidification using 550ul of 1M HCl. Saponified samples were then
213 extracted twice with 1.5ml of Hexanes, taken to dryness under gaseous N_2, and derivatized as
214 above. Derivatized TFA samples were resuspended in 267ul hexanes for injection into the
215 GC/MS. For $^{13}C_2$-acetate tracer samples, 50 ul of the resuspended total lipids was transferred to a
216 new Teflon lined screw cap glass tube, mixed with (66.7 ng) $^{2}D_{31}$-palmitate internal standard and
217 taken to dryness under gaseous N_2. Samples were saponified, extracted, and derivatized as
218 above. Derivatized samples were resuspended in 267ul hexanes for injection. For the NEFA, TFA
219 and tracer fractions, 1ul of pentafluorbenzyl-FA derivatives was injected and data were collected
220 on the GC-MS (8890 GC, 5977B MSD, Agilent) DB-1MS UI column (122-0112UI, Agilent)
221 with the following run program: 80C hold for 3 minutes, 30C/minute ramp to 125C, no hold,
222 25C ramp to 320C and hold for 2 minutes. The flow for the methane carrier gas was set at
223 1.5mL/minute. Data were acquired in full scan negative chemical ionization mode to identify
224 fatty acids of acyl chain length from 8 to 22 carbons. Peak areas of the analyte or of the standard
225 were measured, and the ratio of the area from the analyte-derived ion to that from the internal
226 standard was calculated (22). $^{13}C_2$-acetate tracer incorporation into palmitic acid was analyzed in
227 two carbon increments from M+2 (257 m/z) to M+16 (271 m/z) relative to the quantitative $^{2}D_{31}$-
228 palmitate internal standard (23-25).
229

230 **Oil Red O Staining**

231 500 mg of Oil Red O (ORO) powder was dissolved in 10 mL of 100% propylene glycol (PEG).
232 While heating ORO/PEG solution in 95C bead bath 90 mL of 100% PEG was added to solution
233 in 10 mL increments with vigorous swirling in between additions. Once ORO/PEG solution
234 cooled to room temperature and before each use, solution was filtered using a Whatman #4 filter
235 paper. For 2D culture: 18 mm glass coverslips were sterilized in 100% ethanol overnight and
236 placed in 6-well plates. Parental and endocrine resistant T47D or UCD4 cells were plated on
237 glass coverslips at $5x10^4$ cells/well in normal media conditions with appropriate maintenance
238 Fulv or 4-OH-Tam drug concentrations. Cells were cultured for 5 days at 37C and 5% CO_2
239 without refreshing medium. After 5 days, cells on coverslips were washed three times with PBS
240 and fixed in 10% buffered formalin for 10 minutes. Formalin was aspirated followed by three
241 more washes of PBS. 1 mL of 100% PEG was added per well for 2 minutes then aspirated to
242 waste. 1 mL of ORO/PEG solution was added to each well and incubated for 15 minutes.
243 ORO/PEG solution was removed to waste, and wells were washed with 60% PEG for 2 minutes.
244 Wells were rinsed with DI H_2O three times and counterstained with 1mL diluted 1:50 Harris
245 Hematoxylin (Fisher Scientific, #SH30-4D) for 10 minutes. Hematoxylin was discarded and
246 wells were washed with DI H_2O until clear. Cells on coverslips were mounted on Fisherbrand™
247 ColorFrost™ Plus Microscope Slides (Fisher Scientific, #12-550-17) using tweezers and
248 aqueous mounting medium (Electron Microscopy Sciences, #17985-10). All slides were imaged
249 at 20X magnification (Olympus, BX40). Neutral lipid stain was quantified on ImageJ as percent
250 area normalized to cell number (4 fields per condition).

251

252 **Immunoblots**

253 All cell lysates for immunoblotting were harvested in RIPA buffer. 100 μg total protein per
254 sample were separated on 7.5% SDS-PAGE gels. Primary antibodies were as follows: FASN
255 (rabbit #3180, Cell Signaling Technologies, 1:1000), ACC1(rabbit #3676, Cell Signaling
256 Technologies, 1:1000), or β-actin (mouse A5441, Sigma, 1:2000). Secondary antibodies were
257 IRDye800CW goat-anti-mouse IgG (926-32210, LiCor Biosciences) and IRDye 680LT goat-
258 anti-rabbit IgG (926-68021, Li-Cor Biosciences) both at 1:5,000. Immunoblots were imaged and
259 analyzed with the Odyssey Infrared Imaging System and Image Studio Lite (LiCor Biosciences).
260

261 **Cell proliferation**

262 Real-time imaging (IncuCyte, Sartorius, Ann Arbor, MI) was used to measure proliferation of
263 cells at × 10 magnification. UCD4 cells were plated at 30,000 cells/well, T47D cells at 20,000
264 cells/well, sextuplicate samples in 96-well plates. For treatments, cells were given vehicle, 10
265 μM TVB-2640 plus 1 μM 4OH-Tam, or 100 nM Fulv on day one. Cells were counted under
266 phase contrast immediately after treatment and subsequently taken every 4 h for 6 days. Counts
267 were calculated as fold change over time zero. Significance was assessed by two-way repeated
268 measures ANOVA for growth curves and t-tests for individual time points.
269

270 **Statistical Analyses.** Statistical analyses were performed with GraphPad Prism 10. Data were
271 plotted as means ± SEM. Two-tailed $p < 0.05$ was considered statistically significant. Asterisks
272 denote levels of statistical significance as determined by one or two-way ANOVA with Tukey's
273 or Dunnett's multiple comparisons test, unpaired two-tailed t-test, one-sided Fisher's exact test,
274 log- rank Mantel-Cox test, Wilcoxon rank sum test, or Chi-squared test for trend. Specific tests

275 used are indicated in the figure legends. All experiments were performed in minimum triplicate
276 biological replicates unless noted otherwise.
277
278
279 **Results**
280
281 **Lipid metabolic pathways are upregulated with endocrine resistance**
282 Endocrine resistant cell lines exhibited reduced proliferation rates compared to their
283 parental counterparts (**Figure S1a-b**). Both T47D and UCD4 endocrine resistant cell lines retain
284 ER expression, albeit at varying levels (**Figure S1c)**. To investigate transcriptional changes
285 associated with resistance, RNA-sequencing was performed on parental and endocrine resistant
286 T47D (TamR, FulvR) and UCD4 (TamR, FulvR, EWD) cells. Principle component analysis
287 revealed distinct gene expression profiles between the parental and endocrine resistant cells, as
288 well as among the different resistant variants (**Figure 1a**). Gene Ontology (GO) analysis of the
289 Biological Processes category identified numerous significantly up- and downregulated terms,
290 with lipid metabolism and associated processes emerging as commonly altered features across
291 the endocrine resistant cell lines (**Figure 1b**). Heatmaps of shared up- and downregulated genes
292 in the Response the Lipid category in T47D (**Figure 1c**) and UCD4 (**Figure 1d**) endocrine
293 resistant cells are depicted. Notably, lipid metabolism was consistently altered, with more
294 pathways and genes upregulated than down regulated, highlighting the role of lipid metabolic
295 reprogramming in endocrine resistance.

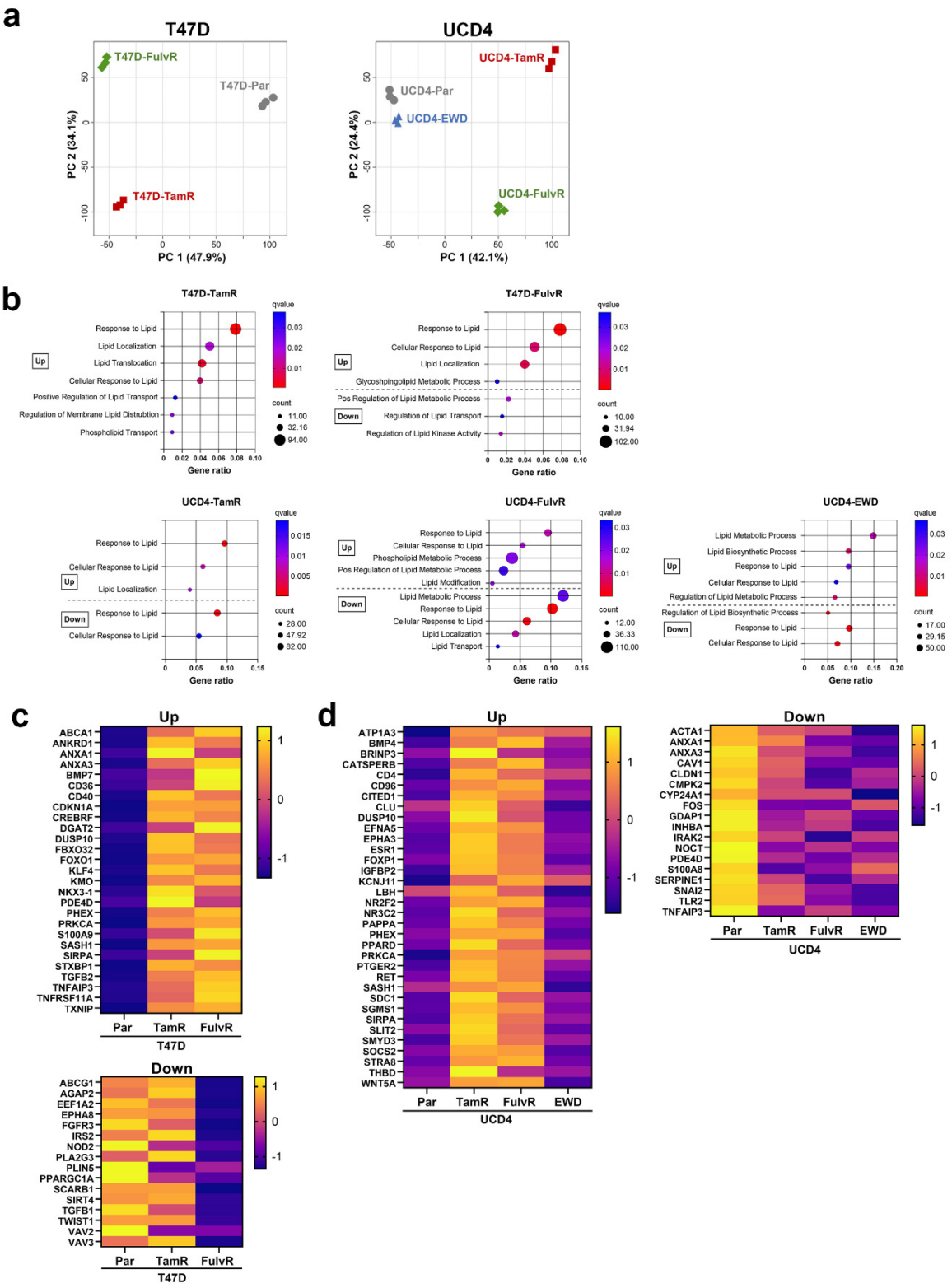
a
T47D
T47D-FulvR
T47D-Par
T47D-TamR
PC 2 (34.1%)
PC 1 (47.9%)
UCD4
UCD4-TamR
UCD4-Par
UCD4-EWD
UCD4-FulvR
PC 2 (24.4%)
PC 1 (42.1%)
b
T47D-TamR
Response to Lipid
Lipid Localization
Lipid Translocation
Cellular Response to Lipid
Positive Regulation of Lipid Transport
Regulation of Membrane Lipid Distrubtion
Phospholipid Transport
Up
Gene ratio
qvalue
count
T47D-FulvR
Response to Lipid
Cellular Response to Lipid
Lipid Localization
Glycoshpingolipid Metabolic Process
Pos Regulation of Lipid Metabolic Process
Regulation of Lipid Transport
Regulation of Lipid Kinase Activity
Down
UCD4-TamR
UCD4-FulvR
UCD4-EWD
Lipid Metabolic Process
Lipid Biosynthetic Process
Phospholipid Metabolic Process
Lipid Modification
Lipid Transport
Regulation of Lipid Metabolic Process
Regulation of Lipid Biosynthetic Process
c
Up
ABCA1
ANKRD1
ANXA1
ANXA3
BMP7
CD36
CD40
CDKN1A
CREBRF
DGAT2
DUSP10
FBXO32
FOXO1
KLF4
KMO
NKX3-1
PDE4D
PHEX
PRKCA
S100A9
SASH1
SIRPA
STXBP1
TGFB2
TNFAIP3
TNFRSF11A
TXNIP
Par
TamR
FulvR
T47D
Down
ABCG1
AGAP2
EEF1A2
EPHA5
FGFR3
IRS2
NOD2
PLA2G3
PLIN5
PPARGC1A
SCARB1
SIRT4
TGFB1
TWIST1
VAV2
VAV3
d
Up
ATP1A3
BMP4
BRINP3
CATSPERB
CD4
CD96
CITED1
CLU
DUSP10
EFNA5
EPHA3
ESR1
FOXP1
IGFBP2
KCNJ11
LBH
NR2F2
NR3C2
PAPPA
PHEX
PPARD
PRKCA
PTGER2
RET
SASH1
SDC1
SGMS1
SIRPA
SLIT2
SMYD3
SOCS2
STRA8
THBD
WNT5A
EWD
UCD4
Down
ACTA1
ANXA1
ANXA3
CAV1
CLDN1
CMPK2
CYP24A1
FOS
GDAP1
INHBA
IRAK2
NOCT
PDE4D
S100A8
SERPINE1
SNAI2
TLR2
TNFAIP3

296

297 **Figure 1: Lipid metabolic pathways are upregulated in endocrine resistant breast cancer**
298 **cells.** a) Principal component analysis (PCA) plots of T47D and UCD4 parental (Par) and
299 endocrine resistant lines based on RNA-sequencing data (triplicate samples). Over representation
300 analysis (ORA) of significantly up- and downregulated genes in lipid pathways ($q<0.05$, log2
301 fold change ≥ 2) from T47D and UCD4 endocrine resistant cells using Gene Ontology (GO)
302 Biological Processes gene sets. T47D-TamR cells showed no significantly downregulated lipid
303 pathways. In some cases, gene cohorts were both significantly up- and downregulated. c and d)
304 Heatmaps of significantly up- and downregulated genes from the "Response to Lipid" process,
305 shared between, (c) T47D-TamR and -FulvR cells (upregulated) and T47D-FulvR cells
306 (downregulated), and (d) UCD4-EWD, -TamR, and -FulvR cells (both up- and downregulated).
307
308 **The global lipidome is altered in endocrine resistant breast cancer cells**.
309 Unbiased lipid mass spectrometry was performed to identify lipidomic changes
310 associated with endocrine resistance in T47D and UCD4 parental lines, as well as their endocrine
311 resistant derivatives. Normalized lipidomic data were analyzed using the publicly available
312 metabolomics tool MetaboAnalyst. Similar to gene expression profiling, PCA analysis of
313 lipidome data showed distinct clustering of samples by parental or endocrine resistant cell type
314 (**Figure 2a-b**). Venn diagrams highlight commonly up- and downregulated lipid analytes in
315 T47D (TamR, FulvR) and UCD4 (TamR, FulvR, EWD) cells (**Figure 2c-d)**. The top 25
316 significantly altered lipid analytes between endocrine resistant and parental cells are depicted in
317 **Figure 2e-f**, with triglycerides and phospholipids among the most affected lipid species. These
318 findings suggest that endocrine resistance in T47D and UCD4 cell lines is characterized by

319 distinct lipidomic reprogramming, with specific alterations in triglycerides and phospholipids

320 potentially playing a critical role in supporting the resistant phenotype.

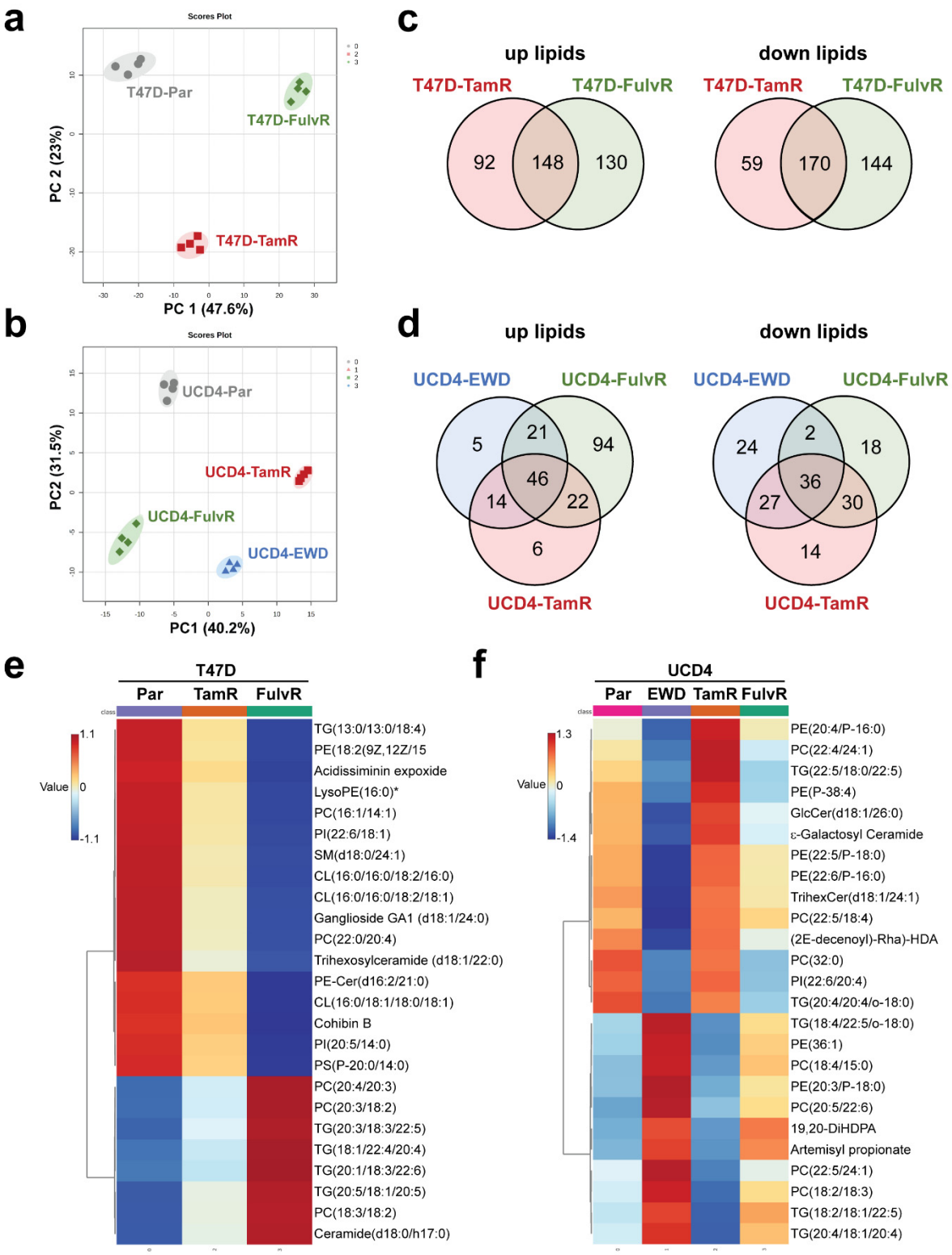
a
Scores Plot
T47D-Par
T47D-FulvR
T47D-TamR
PC 2 (23%)
PC 1 (47.6%)
b
Scores Plot
UCD4-Par
UCD4-TamR
UCD4-FulvR
UCD4-EWD
PC2 (31.5%)
PC1 (40.2%)
c
up lipids
T47D-TamR
T47D-FulvR
92
148
130
down lipids
T47D-TamR
T47D-FulvR
59
170
144
d
up lipids
UCD4-EWD
UCD4-FulvR
UCD4-TamR
5
21
94
46
14
22
6
down lipids
UCD4-EWD
UCD4-FulvR
UCD4-TamR
24
2
18
36
27
30
14
e
T47D
Par
TamR
FulvR
Value
1.1
0
-1.1
TG(13:0/13:0/18:4)
PE(18:2(9Z,12Z/15
Acidissiminin expoxide
LysoPE(16:0)*
PC(16:1/14:1)
PI(22:6/18:1)
SM(d18:0/24:1)
CL(16:0/16:0/18:2/16:0)
CL(16:0/16:0/18:2/18:1)
Ganglioside GA1 (d18:1/24:0)
PC(22:0/20:4)
Trihexosylceramide (d18:1/22:0)
PE-Cer(d16:2/21:0)
CL(16:0/18:1/18:0/18:1)
Cohibin B
PI(20:5/14:0)
PS(P-20:0/14:0)
PC(20:4/20:3)
PC(20:3/18:2)
TG(20:3/18:3/22:5)
TG(18:1/22:4/20:4)
TG(20:1/18:3/22:6)
TG(20:5/18:1/20:5)
PC(18:3/18:2)
Ceramide(d18:0/h17:0)
f
UCD4
Par
EWD
TamR
FulvR
Value
1.3
0
-1.4
PE(20:4/P-16:0)
PC(22:4/24:1)
TG(22:5/18:0/22:5)
PE(P-38:4)
GlcCer(d18:1/26:0)
ε-Galactosyl Ceramide
PE(22:5/P-18:0)
PE(22:6/P-16:0)
TrihexCer(d18:1/24:1)
PC(22:5/18:4)
(2E-decenoyl)-Rha)-HDA
PC(32:0)
PI(22:6/20:4)
TG(20:4/20:4/o-18:0)
TG(18:4/22:5/o-18:0)
PE(36:1)
PC(18:4/15:0)
PE(20:3/P-18:0)
PC(20:5/22:6)
19,20-DiHDPA
Artemisyl propionate
PC(22:5/24:1)
PC(18:2/18:3)
TG(18:2/18:1/22:5)
TG(20:4/18:1/20:4)

321

322 **Figure 2: The lipid profile is altered in endocrine resistant breast cancer cells.** a-b) Principal
323 component analysis (PCA) plots of T47D (a) and UCD4 (b) parental (Par) and endocrine
324 resistant cell samples (quadruplicate) profiled by mass spectrometry-based lipidomics. c-d) Venn
325 diagrams of significantly altered lipid analytes (up- and downregulated, $q<0.05$) in T47D-TamR
326 and -FulvR (c) and UCD4-TamR, -FulvR, and -EWD cells (d) compared to Par cells. e-f)
327 Heatmaps of the top 25 significantly altered shared lipid analytes (up- or downregulated, PLS-
328 DA VIP supervised clustering) between, (e) T47D-TamR and -FulvR cells, and (f) UCD4-TamR,
329 -FulvR, and -EWD cells compared to Par cells. Plots were generated using MetaboAnalyst.
330

331 **Lipid storage is increased during endocrine resistance**

332 To evaluate the potential function of the observed global lipidome changes, we used
333 Lipid Ontology (LION), a publicly available resource that groups analytes within lipidomic data
334 sets by lipid class and function (26). LION heatmap analysis on T47D and UCD4 endocrine
335 resistant compared to parental cells clustered significant analytes into lipid signatures (**Figure**
336 **S2a-b**). The lipid signature containing neutral storage lipids was the most consistently
337 upregulated among endocrine resistant sublines in both T47D and UCD4 cell lines (**Figure 3a-**
338 **b**). These include glycerolipids, triglycerides, lipid droplets, and lipid storage.

339 To further explore lipid storage, we conducted Oil Red O (ORO) neutral lipid staining on
340 parental and endocrine resistant cell lines (**Figure 3c**). A synthetic progesterone analog
341 (promegestone, R5020) was used as a positive control for inducing LD formation (8). T47D and
342 UCD4 parental cell lines displayed basal positive staining for LDs, which was visibly enhanced
343 with R5020 treatment. All endocrine resistant cells showed significantly increased LD staining
344 compared to parental controls (**Figure 3d**). Short term (72 h) treatment of T47D cells with Tam

345 and Fulv did not significantly increase LDs, suggesting that LD accumulation is a feature of
346 acquired resistance (**Figure S3**). To assess whether endocrine resistant cells utilize FAO, a
347 Seahorse Palmitate Oxidation FAO assay was performed on parental and endocrine resistant cell
348 lines (**Figure S4**). FAO was generally decreased in endocrine resistant cells, except for T47D-
349 TamR cells, which showed a modest increase. Overall, our findings indicate that increased LD
350 storage is a consistent feature of acquired endocrine resistance in breast cancer cells.

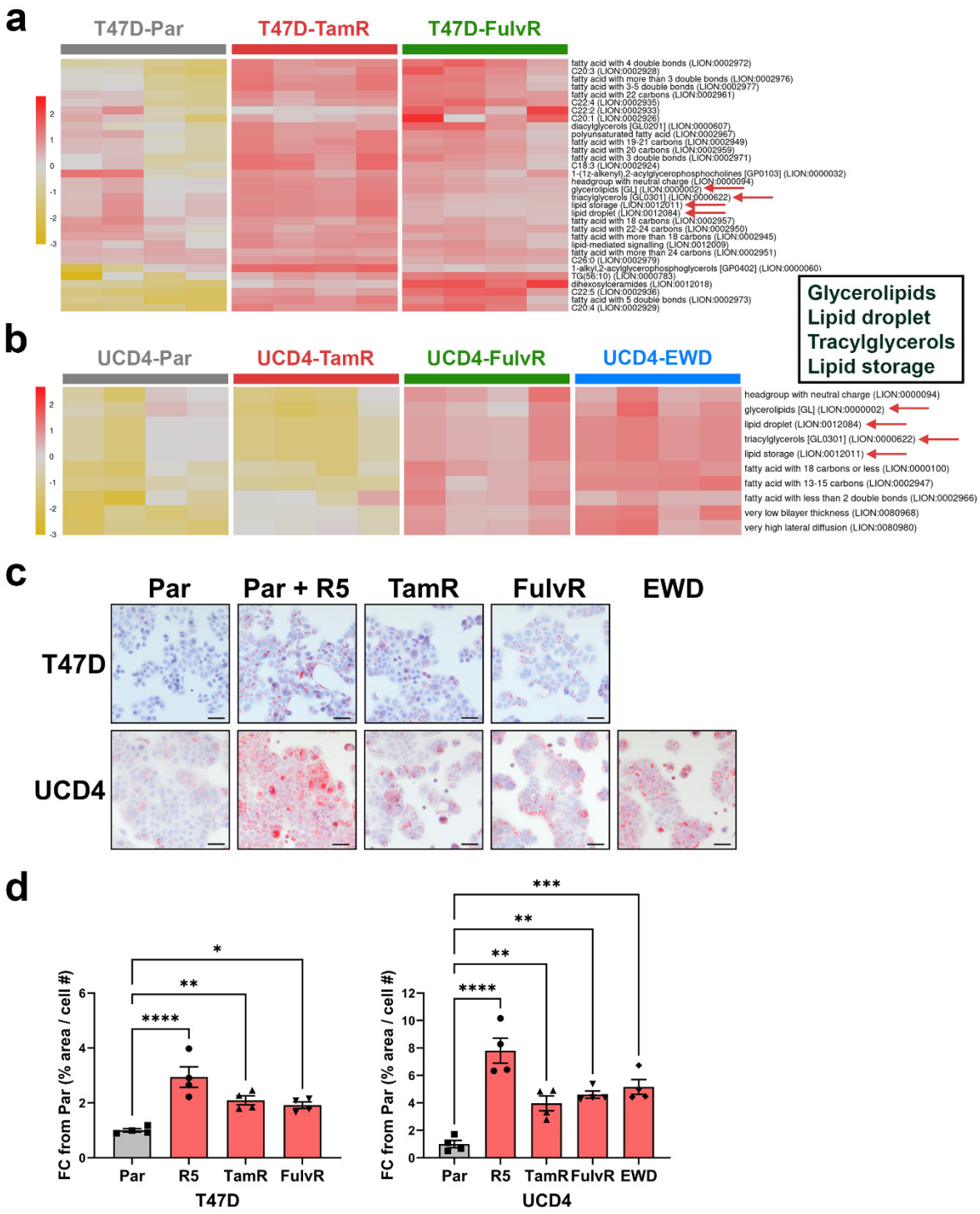
a
T47D-Par
T47D-TamR
T47D-FulvR
fatty acid with 4 double bonds (LION:0002972)
C20:3 (LION:0002928)
fatty acid with more than 3 double bonds (LION:0002976)
fatty acid with 3-5 double bonds (LION:0002977)
fatty acid with 22 carbons (LION:0002961)
C22:4 (LION:0002935)
C22:2 (LION:0002933)
C20:1 (LION:0002926)
diacylglycerols [GL0201] (LION:0000607)
polyunsaturated fatty acid (LION:0002967)
fatty acid with 19-21 carbons (LION:0002949)
fatty acid with 20 carbons (LION:0002959)
fatty acid with 3 double bonds (LION:0002971)
C18:3 (LION:0002924)
1-(1z-alkenyl),2-acylglycerophosphocholines [GP0103] (LION:0000032)
headgroup with neutral charge (LION:0000094)
glycerolipids [GL] (LION:0000002)
triacylglycerols [GL0301] (LION:0000622)
lipid storage (LION:0012011)
lipid droplet (LION:0012084)
fatty acid with 18 carbons (LION:0002957)
fatty acid with 22-24 carbons (LION:0002950)
fatty acid with more than 18 carbons (LION:0002945)
lipid-mediated signalling (LION:0012009)
fatty acid with more than 24 carbons (LION:0002951)
C26:0 (LION:0002979)
1-alkyl,2-acylglycerophosphoglycerols [GP0402] (LION:0000060)
TG(58:10) (LION:0000783)
dihexosylceramides (LION:0012018)
C22:5 (LION:0002936)
fatty acid with 5 double bonds (LION:0002973)
C20:4 (LION:0002929)
Glycerolipids
Lipid droplet
Tracylglycerols
Lipid storage
b
UCD4-Par
UCD4-TamR
UCD4-FulvR
UCD4-EWD
headgroup with neutral charge (LION:0000094)
glycerolipids [GL] (LION:0000002)
lipid droplet (LION:0012084)
triacylglycerols [GL0301] (LION:0000622)
lipid storage (LION:0012011)
fatty acid with 18 carbons or less (LION:0000100)
fatty acid with 13-15 carbons (LION:0002947)
fatty acid with less than 2 double bonds (LION:0002966)
very low bilayer thickness (LION:0080968)
very high lateral diffusion (LION:0080980)
c
Par
Par + R5
TamR
FulvR
EWD
T47D
UCD4
d
FC from Par (% area / cell #)
Par
R5
TamR
FulvR
T47D
EWD
UCD4

353 **Figure 3: Endocrine-resistant breast cancer cells increase cytoplasmic lipid storage.**
354 a-b) Heatmaps of the Lipid Storage LION signature for T47D (a) and UCD4 (b) parental (Par)
355 and endocrine resistant cells based on lipidomics data. Scale bars represent the mean z-score.
356 Selected terms, with their names and IDs, are displayed on the right. Red arrows highlight
357 analytes in the lipid storage signatures. The box on the right indicates the corresponding LION
358 pathway annotations. c) Oil Red O (ORO) staining of T47D and UCD4 parental (Par) and
359 endocrine resistant cells. 5 x 10^4 cells were plated on glass coverslips in the presence of their
360 respective drugs. Positive control cells were treated with 10 nM promegestone (R5). After 5
361 days, cells were formalin fixed, stained with ORO and imaged by light microscopy. Scale bars,
362 50 μM. d) Quantification of ORO staining using ImageJ software (4 fields per slide), expressed
363 as ORO-positive area normalized to cell number. Fold changes from Par are shown as mean ±
364 SEM. One-way ANOVA compares endocrine resistant to Par cells. *P<0.05; **P<0.01;
365 ***P<0.001; ****P<0.0001.
366
367 **TVB-2640 inhibits FASN activity and reduces lipid droplet accumulation in most**
368 **endocrine-resistant breast cancer cells**
369 Enhanced lipid storage can indicate increased FA abundance, either through the *de novo*
370 biosynthesis or FA uptake. We assessed levels of the two rate limiting enzymes in de novo FA
371 synthesis, FASN and Acetyl-CoA Carboxylase 1 (ACC1), by immunoblotting (**Figures 4a & S5**
372 (full blot images). FASN expression was largely unchanged in endocrine resistant compared to
373 parental cells, with an increase observed in UCD4-EWD (1.9 fold) cells. ACC1 levels were
374 similarly unaltered in endocrine resistant cells (0.9-1.2 fold changes). Furthermore,
375 phosphorylation of ACC1 (inactive state) did not significantly differ between parental and

376 endocrine resistant cells (**Figure S6**), suggesting that ACC1 remains in an active state during
377 endocrine resistance. To assess FASN activity, we performed $^{13}C_2$-acetate stable isotope tracing
378 and lipid mass spectrometry to quantify isotope incorporation into palmitate (C16), the primary
379 product of FASN, in T47D-parental cells (with or without R5020 treatment), as well as -TamR,
380 and -FulvR cells (**Figure 4b**). R5020-treated parental cells (positive control), -TamR, and -FulvR
381 cells exhibited significantly higher isotope incorporation into palmitate compared to vehicle
382 treated parental cells, indicating elevated FASN enzymatic activity endocrine resistant cells.
383 Treatment with TVB-2640 completely ablated isotope incorporation into palmitate in all tested
384 conditions, including T47D parental (with or without R5020, -TamR, and -FulvR cells,
385 confirming the inhibitor's potency in blocking FASN enzymatic inhibition.
386 To evaluate whether FASN inhibition affects lipid accumulation, we performed ORO
387 staining on T47D and UCD4 parental and endocrine resistant cells, with or without TVB-2640
388 treatment (**Figure 4c)**. In parental cells, TVB-2640 treatment blocked R5020-induced LD
389 formation in both T47D and UCD4 cells (**Figure 4c-d**). Among the endocrine resistant
390 derivatives, TVB-2640 significantly reduced LD accumulation in all cell lines except T47D-
391 FulvR, where a significant increase was observed. Interestingly TVB-2640 treatment also
392 increased LD abundance in UCD4-parental cells. Additionally, a third endocrine resistant cell
393 line, UCD65-TamR, exhibited significantly higher LD staining compared to parental cells, which
394 was effectively reduced by TVB-2640 (**Figure S3**). Together, these results demonstrate that
395 while TVB-2640 is broadly effective in reducing LD accumulation, its impact is variable,
396 depending on the cell lines and mode of resistance.

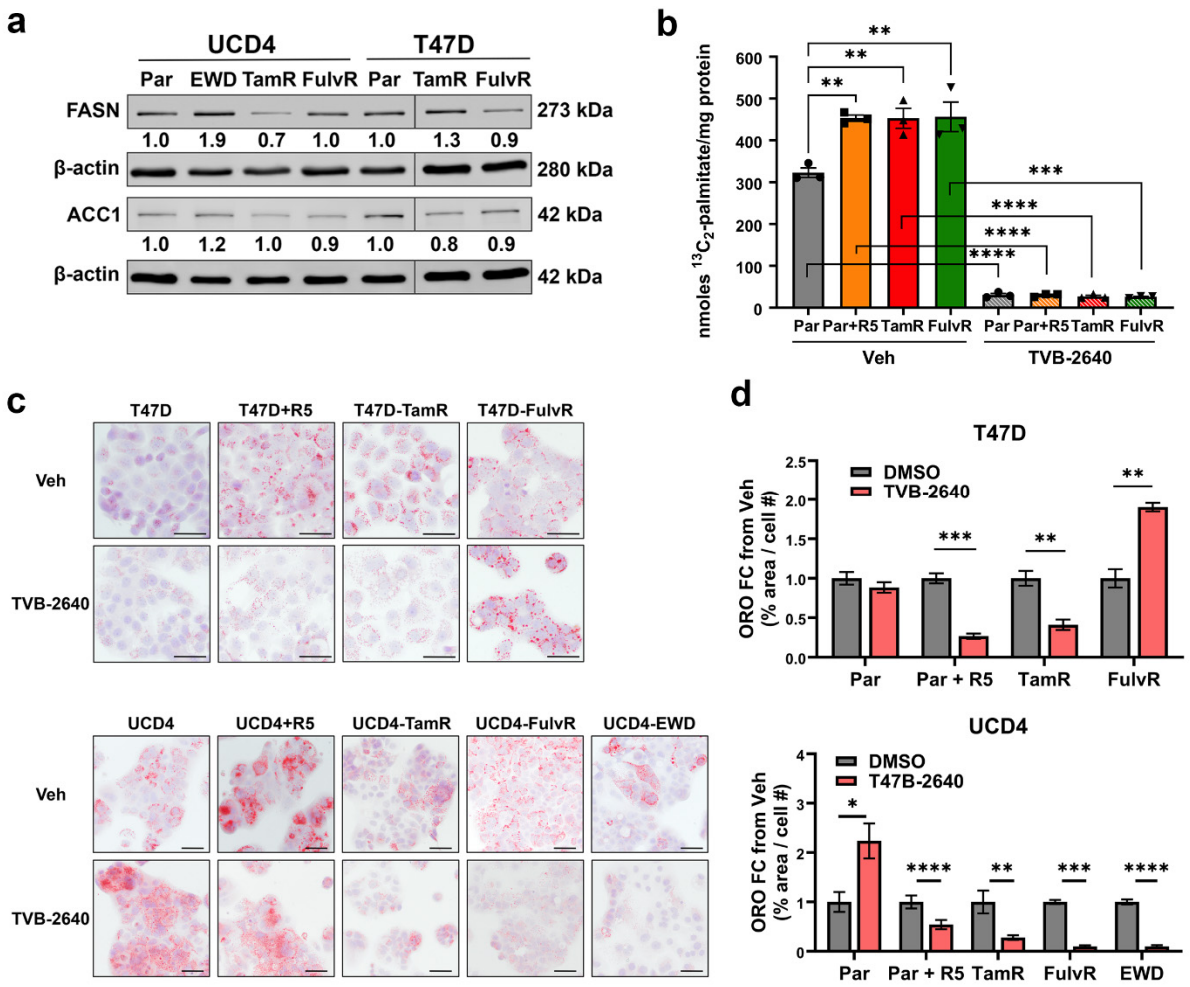

Figure 4: Elevated FASN activity and lipid accumulation in endocrine resistant breast cancer cells. a) Immunoblots of FASN and ACC1 in parental (Par) and endocrine resistant T47D and UCD4 cells. Bands were normalized to β-actin, and fold change over parental is indicated. Removed lanes are denoted by a band. b) Quantification of $^{13}C_2$ acetate tracer incorporation into palmitate in T47D parental (Par), -TamR, and -FulvR cells. Positive control cells were treated with 10 nM promegestone (R5) on day zero. Cells were treated with vehicle (DMSO) or 10 uM TVB-2640 for 72 h. c) ORO staining of T47D (top) and UCD4 (bottom) parental and endocrine resistant cells with or without TVB-2640. 5 x 10^4 parental and endocrine resistant cells were

406 plated on glass coverslips. Positive control cells were treated with 10 nM promegestone (R5) on
407 day one. Cells were treated with vehicle (DMSO) or 10 uM TVB-2640 for 5 days. Scale bars, 50
408 µm. d) Quantification of ORO staining using ImageJ software (4 fields per slide), plotted as the
409 ratio of ORO-positive area over cell number. Fold change from parental (Par) is indicated
410 plus/minus SEM. One-way ANOVA compares endocrine resistant to parental cells. **P<0.01;
411 ***P<0.0001; ****P<0.0001.
412

413 **Limited impact of the FASN inhibitor TVB-2640 on the growth of endocrine-resistant**
414 **breast cancer cells**

415 Since TVB-2640 effectively inhibited FASN activity, we assessed its impact on the
416 proliferation of endocrine resistant cells. Parental and endocrine resistant derivatives of T47D
417 and UCD4 cells were treated with TVB-2640 at the same dose used in tracing studies (10 µM)
418 and monitored using IncuCyte live cell analysis (**Figure 5**). Minimal differences in proliferation
419 were observed at 72 h, the timepoint used for tracing studies, with fold changes of less than 1.2
420 in T47D-TamR and -FulvR cells and no significant changes in UCD4 endocrine resistant
421 compared to vehicle treated parental cells (**Figure 5a-b**). By 6 days post-treatment, proliferation
422 of T47D cell lines was modestly reduced, with a significant >1.5 fold reduction observed in
423 parental, TamR, and FulvR cells (**Figure 5c**). However, UCD4 cells remained largely unaffected,
424 with no significant changes in proliferation across 6 days of treatment (**Figure 5d**). To evaluate
425 whether higher doses of TVB-2640 could have a greater impact on cell growth, IC50 analyses
426 were performed in T47D and UCD4 parental and endocrine resistant cells (**Figure S8a-b**). T47D
427 cells displayed IC50 values ranging between 9-19 µM, indicating sensitivity at doses slightly
428 above the tracing study concentration. UCD4 cell lines did not achieve efficient cytotoxicity at

429 the highest solvent-compatible dose tested, and IC50 values could not be determined. Similarly,
430 UCD65 cells exhibited no significant sensitivity to TVB-2640, except at the highest dose tested
431 (100 µM) (**Figure S8c**). These findings demonstrate that while TVB-2640 effectively inhibits
432 FASN activity and frequently reduces LD accumulation, these effects do not consistently
433 translate into significant growth inhibition in endocrine resistant breast cancer cells.

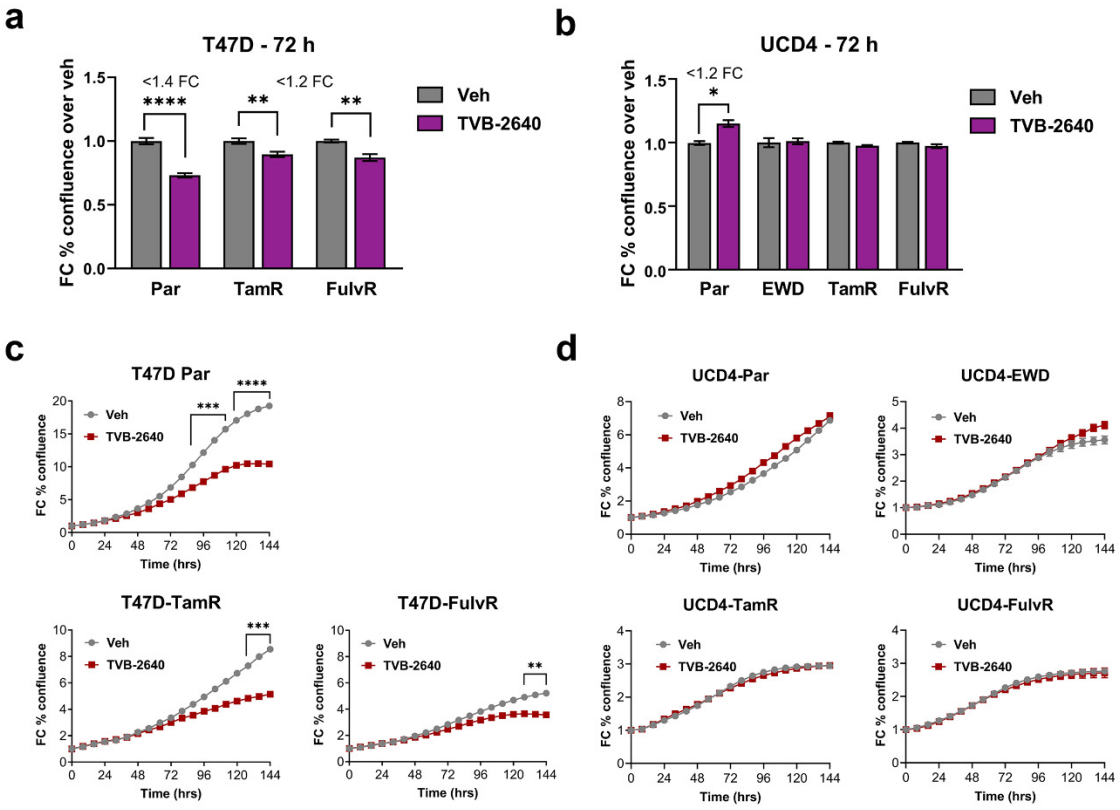

434

435 **Figure 5: Minimal impact of the FASN inhibitor TVB-2640 on endocrine resistant breast**
436 **cancer cell growth.** a-b) fold change (FC) bar graphs of percent confluence at the 72 h timepoint
437 for T47D (a) and UCD4 (b) parental (Par) and endocrine resistant cells treated with vehicle (Veh,
438 DMSO) or 10 uM TVB-2640. FC is indicated where significant, based on a t-test comparing
439 treatment to Veh; *P<0.05; **P<0.01; ****P<0.0001. c-d) Proliferation growth curves of T47D
440 (c) and UCD4 (d) parental (Par) and endocrine resistant cells treated with vehicle (DMSO) or 10

441 uM TVB-2640 over 6 days. FC from timepoint 0 was calculated using the IncuCyte imaging
442 system. Two-way ANOVA significance was calculated, with significance indicated at timepoints
443 with ≥1.5 FC. **P<0.01, ***P<0.001; ****P<0.0001.
444
445 **Endocrine resistance increases lipids with unsaturated acyl chains**
446 Our LION enrichment analysis revealed a higher abundance of lipids with increased
447 desaturation, particularly evident in T47D endocrine resistant cells (**Figure S2**). To explore this
448 in greater detail, significantly altered lipid analytes were categorized based on their degree of
449 desaturation, defined as 6-12 double bonds (**Figure 6a**). The top ten up- and downregulated lipid
450 species are for T47D (TamR, FulvR) and UCD4 (TamR, FulvR, EWD) cells compared to
451 parental cells are shown. In general, highly desaturated lipids were more frequently upregulated
452 than downregulated in endocrine resistant cells. To compare the absolute abundance of
453 desaturated lipids, cumulative lipid species detected by lipidomics were stratified by the of
454 unsaturation (≥6 double bonds) (**Figure 6b**). T47D-TamR and -FulvR cells showed significant
455 increases in total lipid species with high degrees of unsaturation, particularly those with ≥10
456 double bonds, while UCD4 endocrine resistant cells exhibited a more bivalent trend. Lipid
457 species with lower saturation were significantly decreased, whereas complex lipids with ≥11
458 double bonds were consistently significantly increased.
459 To further investigate PUFA abundance, we analyzed PUFA levels in T47D parental, -
460 TamR, and -FulvR cells from our tracing studies, where acyl chains were chemically liberated.
461 Long chain (LC) PUFAs (≥18 carbons), n-6 PUFAs (e.g. arachidonic acid, AA) and n-3 PUFAs
462 (e.g eicosapentaeonic acid, EPA, and docosahexanoic acid, DHA) were significantly increased in
463 T47D-TamR and -FulvR compared to parental cells (**Figure 6c**). Interestingly, FASN inhibition

464 with TVB-2640 further increased LC, n-3, and n-6 PUFA levels, specifically in T47D-FulvR
465 cells, which also exhibited increased lipid accumulation following drug treatment (**Figure 4c-d**).
466 No differences in LC, n-6, or n-3 PUFA levels were observed with R5020 treatment, either in the
467 presence or absence of TVB-2640, indicating that elevated PUFA synthesis is a unique feature of
468 endocrine resistant breast cancer cells. Together, these findings demonstrate that LC-PUFAs are
469 specifically increased in endocrine resistant compared to parental cells, implicating desaturase
470 activity as a potential alternate target in drug-resistant breast cancer.

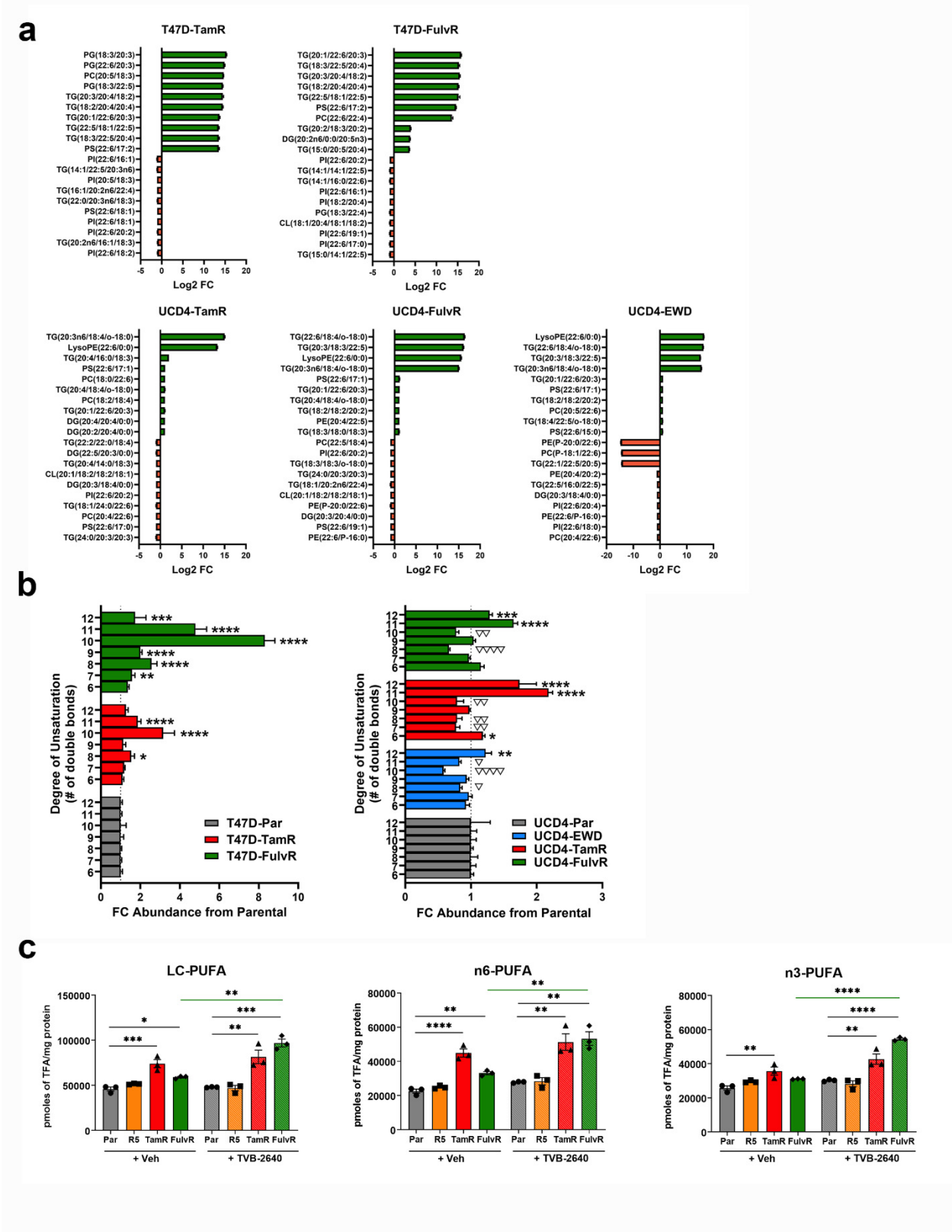
a
T47D-TamR
T47D-FulvR
UCD4-TamR
UCD4-FulvR
UCD4-EWD
Log2 FC
b
Degree of Unsaturation (# of double bonds)
FC Abundance from Parental
T47D-Par
T47D-TamR
T47D-FulvR
UCD4-Par
UCD4-EWD
UCD4-TamR
UCD4-FulvR
c
LC-PUFA
n6-PUFA
n3-PUFA
pmoles of TFA/mg protein
Par
R5
TamR
FulvR
+ Veh
+ TVB-2640

471

472 **Figure 6: Lipid analytes with highly unsaturated acyl chains are increased in endocrine**
473 **resistant breast cancer cells.** a) Top ten upregulated and downregulated lipid analytes with ≥6
474 double bonds in T47D (top) and UCD4 (bottom) endocrine resistant cells compared to parental
475 cells. Log2 fold changes ± SEM are shown, with species listed on the left. b) Fold changes in
476 absolute concentrations of lipid analytes grouped by degree of saturation (≥6 double bonds) in
477 T47D (left) and UCD4 (right) endocrine resistant cells compared to parental (Par). One-way
478 ANOVA was applied to compare endocrine resistant to parental cells. Upregulated are indicated
479 by *P<0.05; **P<0.01; ***P<0.0001; ****P<0.0001. Downregulated are indicated by ▽P<0.05,
480 ▽▽P<0.01, ▽▽▽▽P<0.001. c) Concentration of long chain (LC), n-6, and n-3 PUFAs in
481 T47D-TamR and -FulvR compared to parental cells, treated with vehicle (Veh, DMSO) or 10 uM
482 TVB2640 for 72 h. Positive control cells were treated with 10 nM promegestone (R5) on day
483 zero. One-way ANOVA compared T47D-TamR and -FulvR, and R- treated cells to Par T47D
484 cells within the Veh and TVB-2640 treated groups. T-tests (green lines) indicate compare
485 treatments ± TVB-2640. *P<0.05; **P<0.01; ***P<0.0001; ****P<0.0001.
486
487
488 **Discussion**
489
490 Lipid metabolic reprogramming is a hallmark of breast cancer and varies across its major
491 subtypes: ER+, HER2+, and TNBC (27). In this study, we focused on aberrant lipid metabolism
492 in ER+HER2− breast cancer during acquisition of endocrine resistance. We found that endocrine
493 resistant breast cancer cells, compared to their sensitive counterparts, commonly increase lipid
494 storage and exhibit lipidomes enriched with PUFAs with ≥6 double bonds. Our data suggest that

495 endocrine resistant cells enhance both de novo FA synthesis and the processing of exogenous
496 FAs into PUFAs. These findings highlight that breast cancer cells adapt to chronic endocrine
497 disruption by activating multiple FA synthesis and processing pathways, and demonstrate that
498 targeting synthesis alone is unlikely to be effective in ER+ endocrine resistant breast cancer.
499 LD accumulation is a common feature of aggressive cancers, although their precise role
500 in tumor progression remains unclear (28). LDs are organelles that are synthesized in the
501 endoplasmic reticulum and are mainly composed of neutral lipid triglycerides and cholesterol
502 esters. These LDs provide triglycerides for energy reserves, membrane synthesis, and signaling.
503 A novel role for LDs in aggressive cancers is their ability to sequester drugs; Schlaepfer et al
504 demonstrated that progestins increase LDs in breast cancer cells, which then sequester taxanes
505 (8). We speculate that LDs may also sequester Tam and Fulv in endocrine resistant cells as both
506 are fat soluble molecules. TamR breast cancer cells have previously been observed to increase
507 LDs (12). Our studies demonstrate that resistance to Tam, Fulv, and EWD are all accompanied
508 by exacerbated lipid storage, suggesting that increased LD production may be a common stress
509 adaptation to chronic endocrine disruption. While TNBC cells typically have higher levels of
510 FAO compared to ER+ cells (29), Ahn et al demonstrated that ER+ TamR breast cancer cells
511 have a FAO gene signature resembling that of TNBC (30). Using a Seahorse FAO assay, we
512 detected a marginal increase in FAO in T47D-TamR cells, with T47D-FulvR and UCD4
513 endocrine resistant lines showing decreased FAO compared to parental cells. Overall, LDs
514 accumulate during endocrine resistance, and these structures have multifaceted roles in FA
515 metabolism and drug resistance.
516 It is well recognized that breast cancer versus normal cells increase FASN driven de novo
517 FA synthesis (6). FASN is a long-studied lipid metabolism target as it is universally increased in

518 breast carcinoma cells and linked to worse prognosis (15, 31, 32). Most preclinical studies have
519 found FASN blockade synergizes with chemotherapy drugs (16). However, investigation of
520 FASN inhibition in the context of endocrine resistance is limited. TVB compounds are reversible
521 imidazopyridine-derived inhibitors of FASN. Since endocrine resistant cells have elevated FASN
522 levels in tandem with increased lipid storage, we tested how the new generation FASN inhibitor
523 TVB-2640 impacted endocrine resistant cells. TVB-2640 effectively decreased FASN activity
524 demonstrated by lack of palmitate synthesis, and mostly decreased LD abundance in treated
525 cells. An exception was T47D-FulvR cells that increased LDs with FASN blockade. In T47D-
526 FulvR cells we noted FASN inhibition increases LC-PUFAs. This suggests that some cells may
527 react to blockade of de novo synthesis by processing essential imported FAs such as alpha-
528 linolenic acid into LC-PUFAs. FASN blockade reduced the growth of all T47D cell lines by 5-6
529 day but not at 3-day time points, indicating a delayed effect, and one that does not coincide
530 universally with LD reduction. TVB-2640 treatment reduced LDs in all UCD4 endocrine
531 resistant cells and UCD65-TamR cells. Interestingly, growth of UCD4 cells was unaffected by
532 TVB-2640, and UCD65 only at cytotoxic doses, suggesting some ER+ cells are not reliant on
533 FASN activity and LDs for their drug resistance. LDs alone are therefore not a reliable read-out
534 of FASN activity. Both the Phase I trial of TVB-2640 and the ongoing Phase II trial (prioritizing
535 advanced HER2+ breast cancers) are in combination with chemotherapy (NCT03179904).
536 Malonyl carnitine, a metabolite of malonyl-CoA, increased in the serum of patients taking TVB-
537 2640, demonstrating in vivo target efficiency (17). The efficacy of TVB drugs in combination
538 with endocrine resistance, despite effective FASN blockade, may have other off target activities.
539 For example, Gruslova et al demonstrated that the closely related FASN inhibitor TVB-3166
540 decreased growth of MCF7-TamR cells potentially through degradation of ER (33). Our data

541 insinuate that blocking de novo FA synthesis in endocrine resistant breast cancer cells may not be
542 sufficient to improve treatment due to well recognized lipid metabolic flexibilities. A recent
543 study found that inhibiting ACC1 to block malonyl-coA synthesis could resensitize long term
544 estrogen deprived breast cancer cells in some contexts, prospectively by blocking peroxisome
545 mediated LC-FA oxidation (34).

546 Our experiments uncovered that endocrine resistant versus parental cells contain a higher
547 content of lipids with increased degrees of unsaturation, particularly PUFAs with greater than
548 nine double bonds. Interestingly, in T47D-FulvR cells, PUFAs increased further upon FASN
549 inhibition. PUFAs provide building blocks for membrane expansion, their synthesis provides
550 energy in the form of NADPH for other metabolic reactions, and they serve as substrates for the
551 synthesis of oxidized signaling lipids. However, excessive storage of PUFAs leaves cells
552 vulnerable to lipid peroxidation, which can trigger cell death through processes such as
553 ferroptosis (35). The enzymes that catalyze the generation of double carbon bonds in FAs are the
554 FA desaturases (FADS). The main FADS in humans include FADS5, otherwise known as
555 Stearoyl-CoA Desaturase (SCD), which produces monounsaturated FAs from C16 and C18 FAs,
556 and FADS1, FADS2, that produce n-6 and n-3 PUFAs from the essential C18 FAs linolenic acid
557 and α-linolenic acid, respectively (36). While most studies have focused on inhibiting SCD,
558 several recent studies have focused on blocking other FADS in cancer. Vriens et al identified that
559 by inhibiting SCD in breast cancer cells (not endocrine resistant), FADS2 compensates by
560 producing the alternative FA sapienate, and FADS2 inhibition could reverse this process (31).
561 Thus, disrupting PUFA synthesis by FADS could be particularly damaging to endocrine resistant
562 cells. We observed other lipid metabolic changes in endocrine resistant cells such as altered

563 membrane lipid content that could also reveal vulnerabilities in endocrine resistance and will
564 require further investigation
565
566 **Conclusions**
567 We demonstrate that breast cancer cells resistant to endocrine therapies have increased FASN
568 activity, PUFAs with >6 double bonds, and lipid storage. Targeting de novo synthesis in the
569 presence of endocrine drugs selectively impacted cell growth and did not correlate with LD
570 reduction, suggesting endocrine resistant breast cancer cells may evade FASN inhibition through
571 other lipid metabolic pathways. This prospectively includes the uptake of essential PUFAs that
572 undergo further elongation and desaturation events and may present a unique vulnerability for
573 targeting desaturation in endocrine resistant breast cancer cells.
574
575 **Abbreviations**
576 ACC: Acetyl CoA carboxylase
577 ER: Estrogen Receptor alpha
578 EWD: Estrogen withdrawal
579 FA: Fatty acid
580 FADS2: Fatty Acid Desaturase 2
581 FASN: Fatty acid synthase
582 FAO: Fatty acid oxidation
583 Fulv: Fulvestrant
584 FulvR: Fulvestrant resistant
585 PUFA: Polyunsaturated fatty acid

586 LC-PUFA: Long chain polyunsaturated fatty acid

587 LD: Lipid droplet

588 ORO: Oil Red O

589 PR: Progesterone receptor

590 SERD: Selective estrogen receptor degrader

591 SERM: Selective estrogen receptor modulator

592 SREBP1: sterol regulatory element-binding transcription factor 1

593 Tam: Tamoxifen

594 TamR: Tamoxifen resistant

595 TNBC: Triple negative breast cancer

596

597 **Declarations**

598

599 **Ethics approval and consent to participate**

600 All animal procedures were approved by the Colorado Institutional Animal Care and Use

601 Committee.

602

603 **Acknowledgements**

604 We thank the University of Colorado School of Pharmacy Mass Spectrometry Facility for their

605 consultation and services. We thank the University of Colorado Cancer Center Bioinformatics

606 and Biostatistics Shared Resource supported by P30CA046934.

607

608 **Author contributions**

A.V.W, P.K., M.C.R., and C.A.S. designed the studies. R.R.V., K.B.H., and M.C.R. conducted lipidomic and tracing studies. A.V.W., D.R., and K.E.C. conducted cell culture experiments. A.V.W, D.R., K.E.C., A.E.L., R.R.V., M.C.R. and C.A.S. conducted all data analysis. A.V.W. and C.A.S. drafted manuscript. D.R., J.F.S, H.M.B., R.R.V., P.K., and M.C.R. reviewed and edited manuscript. The project was supervised and funded by M.C.R. and C.A.S. All authors have read and agreed to the published version of the manuscript.

Funding

This work was supported by National Cancer Institute grants R01CA140985 (C.A.S.) 1F31CA261053 (A.V.W.), and R01CA258766 (P.K), the Breast Cancer Research Foundation 23-144 (C.A.S.), and the Cancer League of Colorado (C.A.S, A.V.W.)

Availability of data and materials

The raw RNA-sequencing data is available in the NCBI Gene Expression Omnibus (GEO Accession GSE281935). The unique cell lines are available to qualified individuals for research purposes through formal request, MTA agreement, and appropriate fee.

Consent for publication

Not applicable.

Competing interests

The authors declare that they have no competing interests.

632 **References**

633

634 1. Siegel RL. Cancer statistics, 2022. CA Cancer J Clin. 2022;72(1):7-33.

635 2. Guan J, Zhou W, Hafner M, Blake RA, Chalouni C, Chen IP, et al. Therapeutic Ligands
636 Antagonize Estrogen Receptor Function by Impairing Its Mobility. Cell. 2019;178(4):949-63
637 e18.

638 3. Pan H, Gray R, Braybrooke J, Davies C, Taylor C, McGale P, et al. 20-Year Risks of Breast-
639 Cancer Recurrence after Stopping Endocrine Therapy at 5 Years. N Engl J Med.
640 2017;377(19):1836-46.

641 4. McAndrew NP, Finn RS. Clinical Review on the Management of Hormone Receptor-Positive
642 Metastatic Breast Cancer. JCO Oncol Pract. 2022;18(5):319-27.

643 5. Varella L, Cristofanilli M. Evaluating Elacestrant in the Management of ER-Positive, HER2-
644 Negative Advanced Breast Cancer: Evidence to Date. Onco Targets Ther. 2023;16:189-96.

645 6. Menendez JA, Lupu R. Fatty acid synthase and the lipogenic phenotype in cancer
646 pathogenesis. Nat Rev Cancer. 2007;7(10):763-77.

647 7. Menendez JA, Papadimitropoulou A, Vander Steen T, Cuyas E, Oza-Gajera BP, Verdura S, et
648 al. Fatty Acid Synthase Confers Tamoxifen Resistance to ER+/HER2+ Breast Cancer.
649 Cancers (Basel). 2021;13(5).

650 8. Schlaepfer IR, Hitz CA, Gijon MA, Bergman BC, Eckel RH, Jacobsen BM. Progestin
651 modulates the lipid profile and sensitivity of breast cancer cells to docetaxel. Mol Cell
652 Endocrinol. 2012;363(1-2):111-21.

653 9. Lopes-Coelho F, Gouveia-Fernandes S, Serpa J. Metabolic cooperation between cancer and
654 non-cancerous stromal cells is pivotal in cancer progression. Tumour Biol.
655 2018;40(2):1010428318756203.
656 10. Blask DE. Circadian stage-dependent inhibition of human breast cancer metabolism and
657 growth by the nocturnal melatonin signal: consequences of its disruption by light at night in
658 rats and women. Integr Cancer Ther. 2009;8(4):347-53.
659 11. Jordan VC. Tamoxifen as the first targeted long-term adjuvant therapy for breast cancer.
660 Endocr Relat Cancer. 2014;21(3):R235-46.
661 12. Hultsch S, Kankainen M, Paavolainen L, Kovanen RM, Ikonen E, Kangaspeska S, et al.
662 Association of tamoxifen resistance and lipid reprogramming in breast cancer. BMC Cancer.
663 2018;18(1):850.
664 13. Du T. Key regulators of lipid metabolism drive endocrine resistance in invasive lobular
665 breast cancer. Breast Cancer Res. 2018;20(1):106.
666 14. Simigdala N. Cholesterol biosynthesis pathway as a novel mechanism of resistance to
667 estrogen deprivation in estrogen receptor-positive breast cancer. Breast Cancer Res.
668 2016;18(1):58.
669 15. Alo PL, Visca P, Botti C, Galati GM, Sebastiani V, Andreano T, et al. Immunohistochemical
670 expression of human erythrocyte glucose transporter and fatty acid synthase in infiltrating
671 breast carcinomas and adjacent typical/atypical hyperplastic or normal breast tissue. Am J
672 Clin Pathol. 2001;116(1):129-34.
673 16. Menendez JA, Lupu R. Fatty acid synthase (FASN) as a therapeutic target in breast cancer.
674 Expert Opin Ther Targets. 2017;21(11):1001-16.

675 17. Falchook G, Infante J, Arkenau HT, Patel MR, Dean E, Borazanci E, et al. First-in-human
676 study of the safety, pharmacokinetics, and pharmacodynamics of first-in-class fatty acid
677 synthase inhibitor TVB-2640 alone and with a taxane in advanced tumors.
678 EClinicalMedicine. 2021;34:100797.
679 18. Koundouros N, Poulogiannis G. Reprogramming of fatty acid metabolism in cancer. Br J
680 Cancer. 2020;122(1):4-22.
681 19. Finlay-Schultz J, Jacobsen BM, Riley D, Paul KV, Turner S, Ferreira-Gonzalez A, et al. New
682 generation breast cancer cell lines developed from patient-derived xenografts. Breast Cancer
683 Res. 2020;22(1):68.
684 20. Gendoo DM, Ratanasirigulchai N, Schroder MS, Pare L, Parker JS, Prat A, et al. Genefu: an
685 R/Bioconductor package for computation of gene expression-based signatures in breast
686 cancer. Bioinformatics. 2016;32(7):1097-9.
687 21. Misra BB. Data normalization strategies in metabolomics: Current challenges, approaches,
688 and tools. Eur J Mass Spectrom (Chichester). 2020;26(3):165-74.
689 22. Varshney R. Neonatal intake of Omega-3 fatty acids enhances lipid oxidation in adipocyte
690 precursors. iScience. 2023;26(1):105750.
691 23. Rudolph MC. Mammalian fatty acid synthase activity from crude tissue lysates tracing
692 (1)(3)C-labeled substrates using gas chromatography-mass spectrometry. Anal Biochem.
693 2012;428(2):158-66.
694 24. Rudolph MC. Thyroid hormone responsive protein Spot14 enhances catalysis of fatty acid
695 synthase in lactating mammary epithelium. J Lipid Res. 2014;55(6):1052-65.

696 25. Rudolph MC. Mammalian fatty acid synthase activity from crude tissue lysates tracing 13C-
697 labeled substrates using gas chromatography mass spectrometry. Analytical Biochemistry.
698 2012;428(2):158-66.
699 26. Molenaar MR, Jeucken A, Wassenaar TA, van de Lest CHA, Brouwers JF, Helms JB.
700 LION/web: a web-based ontology enrichment tool for lipidomic data analysis. Gigascience.
701 2019;8(6).
702 27. Monaco ME. Fatty acid metabolism in breast cancer subtypes. Oncotarget.
703 2017;8(17):29487-500.
704 28. Beloribi-Djefaflia S, Vasseur S, Guillaumond F. Lipid metabolic reprogramming in cancer
705 cells. Oncogenesis. 2016;5(1):189.
706 29. Camarda R, Zhou AY, Kohnz RA, Balakrishnan S, Mahieu C, Anderton B, et al. Inhibition of
707 fatty acid oxidation as a therapy for MYC-overexpressing triple-negative breast cancer. Nat
708 Med. 2016;22(4):427-32.
709 30. Ahn S. Metabolomic Rewiring Promotes Endocrine Therapy Resistance in Breast Cancer.
710 Cancer Res. 2024;84(2):291-304.
711 31. Vriens K, Christen S, Parik S, Broekaert D, Yoshinaga K, Talebi A, et al. Evidence for an
712 alternative fatty acid desaturation pathway increasing cancer plasticity. Nature.
713 2019;566(7744):403-6.
714 32. Alò PL. Fatty acid synthase (FAS) predictive strength in poorly differentiated early breast
715 carcinomas. Tumori. 1999;85(1):35-40.
716 33. Gruslova A, McClellan B, Balinda HU, Viswanadhapalli S, Alers V, Sareddy GR, et al.
717 FASN inhibition as a potential treatment for endocrine-resistant breast cancer. Breast Cancer
718 Res Treat. 2021;187(2):375-86.

719 34. Bacci M. Acetyl-CoA carboxylase 1 controls a lipid droplet-peroxisome axis and is a
720 vulnerability of endocrine-resistant ER(+) breast cancer. Sci Transl Med. 2024;16(736):9874.
721 35. Bobinski R, Dutka M, Pizon M, Waksmanska W, Pielesz A. Ferroptosis, Acyl Starvation, and
722 Breast Cancer. Mol Pharmacol. 2023;103(3):132-44.
723 36. Lee JM. Fatty Acid Desaturases, Polyunsaturated Fatty Acid Regulation, and
724 Biotechnological Advances. Nutrients. 2016;8(1).
725